International Tables for Crystallography (2006). Vol. C, Section 4.2.3.1, pp. 213–214.

4.2.3. X-ray absorption spectra (by D. C. Creagh)

4.2.3.1. *Introduction*

4.2.3.1.1. *Definitions*

This section deals with the manner in which the photon scattering and absorption cross sections of an atom varies with the energy of the incident photon. Further information concerning these cross sections and tables of the X-ray attenuation coefficients are given in Section 4.2.4. Information concerning the anomalous-dispersion corrections is given in Section 4.2.6.

When a highly collimated beam of monoenergetic photons passes through a medium of thickness t, it suffers a decrease in intensity according to the relation

$$I = I_0 \exp(-\mu_l t), \tag{4.2.3.1}$$

where μ_l is the linear attenuation coefficient. Most tabulations express μ_l in c.g.s. units, μ_l having the units cm^{-1}.

An alternative, often more convenient, way of expressing the decrease in intensity involves the measurement of the mass per unit area m_A of the specimen rather than the specimen thickness, in which case equation (4.2.3.1) takes the form

$$I = I_0 \exp[-(\mu/\rho)m_A], \tag{4.2.3.2}$$

where ρ is the density of the material and (μ/ρ) is the mass absorption coefficient. The linear attenuation coefficient of a medium comprising atoms of different types is related to the mass absorption coefficients by

$$\mu_l = \rho \sum_i g_i(\mu/\rho)_i, \tag{4.2.3.3}$$

where g_i is the mass fraction of the atoms of the ith species for which the mass absorption coefficient is $(\mu/\rho)_i$. The summation extends over all the atoms comprising the medium. For a crystal having a unit-cell volume of V_c,

$$\mu_l = \frac{1}{V_c} \sum \sigma_i, \tag{4.2.3.4}$$

where σ_i is the photon scattering and absorption cross section. If σ_i is expressed in terms of barns/atom then V_c must be expressed in terms of Å^3 and μ_l is in cm^{-1}. (1 barn = 10^{-28} m^2.)

The mass attenuation coefficient μ/ρ is related to the total photon–atom scattering cross section σ according to

$$\begin{aligned}\frac{\mu}{\rho}(\text{cm}^2/\text{g}) &= (N_{\rm A}/M)\sigma\,(\text{cm}^2/\text{atom})\\ &= (N_{\rm A}/M) \times 10^{-24}\sigma\,(\text{barns/atom}),\end{aligned} \tag{4.2.3.5}$$

where $N_{\rm A}$ = Avogadro's number = 6.0221367 (36) × 10^{23} atoms/gram atom (Cohen & Taylor, 1987) and M = atomic weight relative to $M(^{12}\text{C})$ = 12.0000.

4.2.3.1.2. *Variation of X-ray attenuation coefficients with photon energy*

When a photon interacts with an atom, a number of different absorption and scattering processes may occur. For an isolated atom at photon energies of less than 100 keV (the limit of most conventional X-ray generators), contributions to the total cross section come from the photo-effect, coherent (Rayleigh) scattering, and incoherent (Compton) scattering.

$$\sigma = \sigma_{\rm pe} + \sigma_R + \sigma_C. \tag{4.2.3.6}$$

The relation between the photo-effect absorption cross section $\sigma_{\rm pe}$ and the X-ray anomalous-dispersion corrections will be discussed in Section 4.2.6.

The magnitudes of these scattering cross sections depend on the type of atom involved in the interactions and on the energy of the photon with which it interacts. In Fig. 4.2.3.1, the theoretical cross sections for the interaction of photons with a carbon atom are given. Values of $\sigma_{\rm pe}$ are from calculations by Schofield (1973), and those for Rayleigh and Compton scattering are from tabulations by Hubbell & Øverbø (1979) and Hubbell (1969), respectively. Note the sharp discontinuities that occur in the otherwise smooth curves. These correspond to photon energies that correspond to the energies of the K and $L_{\rm I}$ $L_{\rm II}$ $L_{\rm III}$ shells of the carbon energies. Notice also that $\sigma_{\rm pe}$ is the dominant interaction cross section, and that the Rayleigh scattering cross section remains relatively constant for a broad range of photon energies, whilst the Compton scattering peaks at a particular photon energy (~ 100 keV). Other interaction mechanisms exist [*e.g.* Delbrück (Papatzacos & Mort, 1975; Alvarez, Crawford & Stevenson, 1958), pair production, nuclear Thompson], but these do not become significant interaction processes for photon energies less than 1 MeV. This section will not address the interaction of photons with atoms for which the photon energy exceeds 100 keV.

4.2.3.1.3. *Normal attenuation, XAFS, and XANES*

The curves shown in Fig. 4.2.3.1 are the result of theoretical calculations of the interactions of an isolated atom with a single photon. Experiments are not usually performed on isolated atoms, however. When experiments are performed on ensembles of atoms, a number of points of difference emerge between the experimental data and the theoretical calculations. These effects arise because the presence of atoms in proximity with one another can influence the scattering process. In short: the total attenuation coefficient of the system is *not* the sum of all the individual attenuation coefficients of the atoms that comprise the system.

Perhaps the most obvious manifestation of this occurs when the photon energy is close to an absorption edge of an atom. In Fig. 4.2.3.2, the mass attenuation of several germanium compounds is plotted as a function of photon energy. The

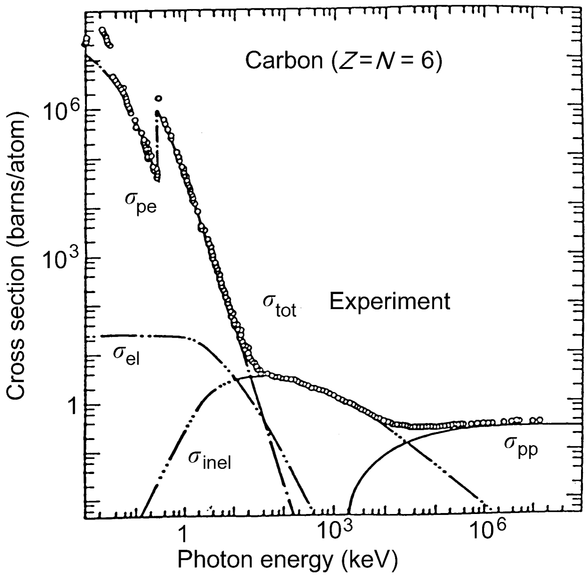

Fig. 4.2.3.1. Theoretical cross sections for photon interactions with carbon showing the contributions of photoelectric, elastic (Rayleigh), inelastic (Compton), and pair-production cross sections to the total cross sections. Also shown are the experimental data (open circles). From Gerstenberg & Hubbell (1982).

energy scale measures the distance from the K-shell edge energy of germanium (11.104 keV). These curves are taken from Hubbell, McMaster, Del Grande & Mallett (1974). Not only does the experimental curve depart significantly from the theoretically predicted curve, but there is a marked difference in the complexity of the curves between the various germanium compounds.

Far from the absorption edge, the theoretical calculations and the experimental data are in reasonable agreement with what one might expect using the sum rule for the various scattering cross sections and one could say that this region is one in which normal attenuation coefficients may be found.

Closer to the edge, the almost periodic variation of the mass attenuation coefficient is called the extended X-ray absorption fine structure (XAFS). Very close to the edge, more complicated fluctuations occur. These are referred to as X-ray absorption near edge fine structure (XANES). The boundary of the XAFS and XANES regions is somewhat arbitrary, and the physical basis for making the distinction between the two will be outlined in Subsection 4.2.3.4.

Even in the region where normal attenuation may be thought to occur, cooperative effects can exist, which can affect both the Rayleigh and the Compton scattering contributions to the total attenuation cross section. The effect of cooperative Rayleigh scattering has been discussed by Gerward, Thuesen, Stibius-Jensen & Alstrup (1979), Gerward (1981, 1982, 1983), Creagh & Hubbell (1987), and Creagh (1987*a*). That the Compton scattering contribution depends on the physical state of the scattering medium has been discussed by Cooper (1985).

Care must therefore be taken to consider the physical state of the system under investigation when estimates of the theoretical interaction cross sections are made.

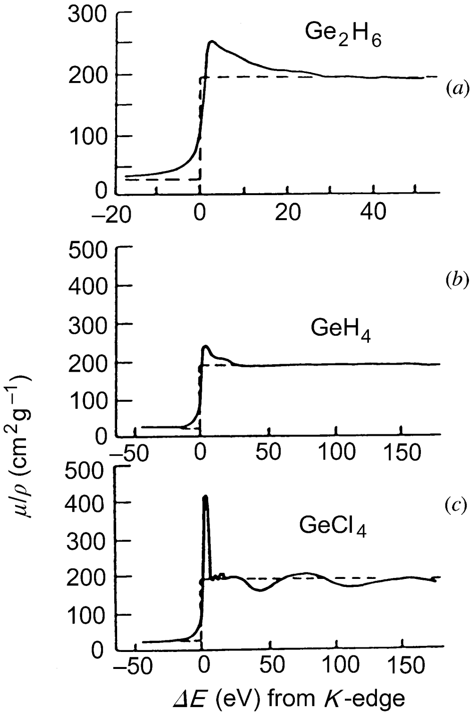

Fig. 4.2.3.2. The dependence of the X-ray attenuation coefficient on energy for a range of germanium compounds, taken in the neighbourhood of the germanium absorption edge (from *IT* IV, 1974).

4.2.3.2. *Techniques for the measurement of X-ray attenuation coefficients*

4.2.3.2.1. *Experimental configurations*

Experimental configurations that set out to determine the X-ray linear attenuation coefficient μ_l or the corresponding mass absorption coefficients (μ/ρ) must have characteristics that reflect the underlying assumptions from which equation (4.2.3.1) was derived, namely:

(i) the incident and transmitted beams are parallel and there is no divergence in the transmitted beam;

(ii) the photons in the incident and transmitted beams have the same energy;

(iii) the specimen is of sufficient thickness.

Because of the considerable discrepancies that often exist in X-ray attenuation measurements (see, for example, *IT* IV, 1974), the IUCr Commission on Crystallographic Apparatus set up a project to determine which, if any, of the many techniques for the measurement of X-ray attenuation coefficients is most likely to yield correct results. In the project, a number of different experimental configurations were used. These are shown in Fig. 4.2.3.3. The configurations used ranged in complexity from that

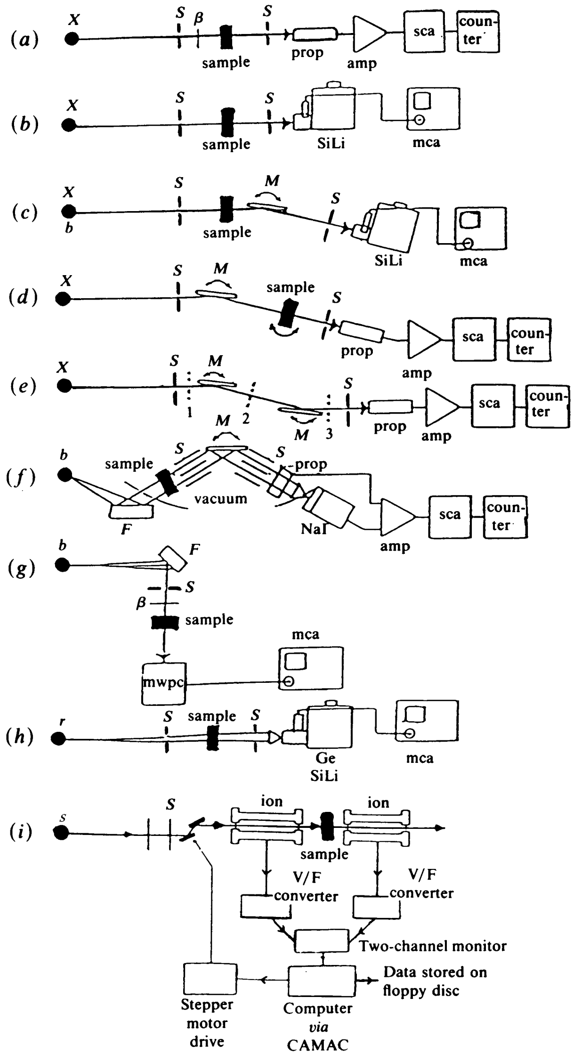

Fig. 4.2.3.3. Schematic representations of experimental apparatus used in the IUCr X-ray Attenuation Project (Creagh & Hubbell, 1987; Creagh, 1985). *X*: characteristic line from sealed X-ray tube; *b*: *Bremsstrahlung* from a sealed X-ray tube; *r*: radioactive source; *s*: synchrotron-radiation source; *β*: *β*-filter for characteristic X-rays; *S*: collimating slits; *M*: monochromator.